Colloid Polym Sci 274:779–787 (1996)

ORIGINAL CONTRIBUTION

Z. Király
L. Turi
I. Dékány
K. Bean
B. Vincent

Van der Waals attraction between Stöber silica particles in a binary solvent system

Received: 18 December 1995
Accepted: 19 January 1996

Dr. Z. Király (✉) · L. Turi · I. Dékány
Department of Colloid Chemistry
Attila József University
Aradi Vértanúk tere 1
6720 Szeged, Hungary

K. Bean · B. Vincent
School of Chemistry
University of Bristol
Cantock's Close
Bristol BS8 1TS, United Kingdom

Abstract Hydrophilic Stöber silica particles are stable in ethanol, but flocculation may be induced by the addition of sufficient cyclohexane. Low-shear rheological measurements indicated non-Newtonian behaviour beyond the critical cyclohexane concentration. The thickness and composition of the solvation layer around the particles were calculated from the adsorption excess isotherm on the basis of a multilayer adsorption model. The composition dependences of the Hamaker constants of the dispersion medium and the adsorption layer were obtained from optical dispersion measurements. A single-sheet, hard-sphere model predicted a weak van der Waals attraction in the ethanolic regime, but a strong attraction in the cyclohexane-rich region, in good accordance with the rheological properties of the dispersions and visual observations.

Key words Silica particles – colloid stability – Hamaker constant – van der Waals potential – adsorption – rheology – SAXS

Introduction

Most academic studies on the colloid stability of submicroscopic solid particles dispersed in liquid media are focused on steric and electrostatic stabilizations. However, interparticular interactions (the relative magnitudes of attractive and repulsive forces between particles) can also be controlled in dispersions which contain neither polymers nor tensides, or even when the role of Coulombic forces is negligible. Evidence seems to be accumulating that the ordering of liquids near a solid surface plays an important role in the stabilization of colloidal dispersions [1, 2]. Kline and Kaler investigated the stability of 2% Ludox silica dispersions in the liquid pair water(1)–2-butoxyethanol(2) [3]. The stabilizing effect of the diffuse electric double layer was found to be dominant in pure water. As the concentration of 2-butoxyethanol was increased, the surface charge was gradually screened out and the role of the Coulombic forces became negligible. Under these circumstances, the stability of the system was dependent on the long-range van der Waals forces and the short-range interactions between the adsorption layers of the colliding particles. Beysens et al. studied the stability behaviour of Stöber silica spheres in the partially miscible binary solvent system water(1)–2,6-lutidine(2) [4, 5]. In the close proximity of the solubility limit of lutidine in water, a thick (3–7 nm) layer of lutidine was formed on the surface of the silica particles (pre-wetting). The mutual attraction between these solvation layers led to reversible flocculation of the particles. Edwards et al. reported on the reversible flocculation of stearylated Stöber silica particles (organophilized by octadecanol) in *n*-alkanes, induced by a variation of temperature [6]. In the stable zone of the phase diagram, i.e., temperature vs. particle concentration diagram, the van der Waals attraction was well overcompensated by the kinetic energy of particle collision, because the difference between the Hamaker constant of the stearyl

Colloid & Polymer Science, Vol. 274, No. 8 (1996)

layer and that of the dispersion medium was sufficiently low. However, a gradual increase or decrease of temperature caused a significant change in the Hamaker constant of the dispersion medium, whereas for the silica particles and the stearyl layer such changes were rather small. As the difference between the Hamaker constants of the medium and the stearyl layer increased, the van der Waals attraction also increased. As a consequence, when either the lower or the upper critical temperature was reached, the system underwent flocculation and unstable zones appeared in the phase diagram. By analogy with the Θ-state (more strictly, the critical state) of polymeric solutions, it may be expected that the stability of colloidal dispersions (at a constant solvent composition) may be influenced not only by an elevation or lowering of the temperature, but also by change of the composition of the dispersion medium (at a constant temperature). Vincent et al. determined the stability phase diagrams of bare and stearylated Stöber silica particles dispersed in ethanol(1)–cyclohexane(2) mixtures [7]. It was established that the organosol, which is stable in cyclohexane, is flocculated by the addition of sufficient ethanol, i.e., when a critical ethanol concentration is reached. In contrast, hydrophilic silica is stable in ethanol (alcosol) and is flocculated beyond a critical cyclohexane concentration. In mixed media, variation of the solvent composition influences not only the Hamaker constant of the medium: as a result of the solid/liquid interfacial interaction, the thickness and composition of the adsorption layer, and hence the Hamaker constant of the interfacial layer, are also affected by the composition of the bulk liquid phase. Dékány et al. reported that the stability of fumed silica in mixed liquid media increases when the Hamaker constants of the lyosphere and the dispersion medium approach each other [8–10]. At the adsorption azeotropic composition, they are identical and the stability becomes maximal. An increase in the thickness of the adsorption layer enhances the stability of the dispersions. In the calculation of the van der Waals interaction pair potential between the particles, the thickness and composition of the adsorption layer appear as a geometric factor and a factor dependent upon the chemical properties, respectively [11–13]. The formation of a thick adsorption layer extending from the solid surface towards the bulk liquid phase, with a gradual approach to the composition of the dispersion medium, may ensure the stability of a disperse system, in accordance with the Ostwald–Buzágh theory of continuity [14, 15]. The present work involves the relation between adsorption and colloid stability in the ethanol(1)–cyclohexane(2)/Stöber silica system, in a continuation of our previous studies on the stability of silica dispersions in binary solvent mixtures [7–10].

Theory

When solid particles of mass m are dispersed in a binary liquid mixture of total amount n^0, the reduced adsorption excess amount of the first component, $n_1^{\sigma(n)}$, at the solid/liquid interface is by definition [16, 17]:

$$n_1^{\sigma(n)} = \frac{n^0}{m}(x_1^0 - x_1)\,, \tag{1}$$

where x_1^0 and x_1 are the initial and equilibrium molar fractions of component 1 in the liquid phase. If the adsorption excess isotherm of the preferentially adsorbed component 1 is of type II in the Schay–Nagy isotherm classification, then the adsorption capacity of pure component 1 can be determined by the Schay–Nagy method, i.e., by extrapolation to zero concentration from the linear region of the isotherm [16, 17]:

$$\lim_{x_1 \to 0} [n_1^{\sigma(n)}] = n_1^{s,0}\,. \tag{2}$$

On the other hand, the Everett-Schay representation of type II isotherms is linear within a wide range of compositions, and the slope of the straight line is the reciprocal of the adsorption capacity [16, 17]:

$$\frac{1}{(d/dx_1)\,[x_1 x_2 / n_1^{\sigma(n)}]} = n_1^{s,0}\,. \tag{3}$$

The average composition of the adsorption layer, x_1^s, for a number t of successive layers [17] is

$$x_1^s = \frac{t x_1 + a_2 \Gamma_1^{(n)}}{t + (a_2 - a_1)\Gamma_1^{(n)}}\,, \tag{4}$$

where a_1 and a_2 are the molar cross-sectional area of the components in a monomolecular adsorption layer, and $\Gamma_1^{(n)}$ is the reduced surface excess concentration. The number of layers, t, may be calculated via one or other of the following formulas, depending on whether an area-filling or a space-filling model is used [16, 17]:

$$t = \frac{a_1 n_1^{s,0}}{a_s} \quad \text{or} \quad t = \frac{v_1 n_1^{s,0}}{a_s \delta_1}\,, \tag{5}$$

where a_s is the specific surface area of the adsorbent (particle), while v_1 and δ_1 are the molar volume and molecular diameter, respectively, of component 1. Accordingly, the thickness of the adsorption layer is

$$\delta = t\delta_1\,. \tag{6}$$

The *minimum* value of t, which is still physically realistic, can also be determined by means of a thermodynamic consistency test, the Rusanov criterion [17]. According to this criterion, thermodynamically consistent results are

obtained when

$$\left(\frac{\partial x_1^s}{\partial x_1}\right)_{T,p} > 0 \quad \text{if } \Gamma_1^{(n)} > 0 \,. \tag{7}$$

Starting with a layer number of $t = 1$, and gradually increasing its value in Eq. (4), the x_1^s vs. x_1 adsorption equilibrium diagram is constructed for each value of t. If this function has an extreme, the value of t must be rejected and further increased. In this way the minimum number of layers is obtained when Rusanov's criterion (7) is first fulfilled.

The average composition of the interfacial layer may also be calculated from a combination of the Ostwald-de Izaguirre and Williams equations [16]:

$$x_1^s = \frac{x_1 n_1^{s,0} + r n_1^{\sigma(n)}}{n_1^{s,0} + (r-1) n_1^{\sigma(n)}} \,, \tag{8}$$

where r is the size ratio of the molecules of the liquid components. This stoichiometric coefficient may be obtained as

$$r = \frac{v_2}{v_1} \quad \text{or} \quad r = \frac{a_2}{a_1} \,, \tag{9}$$

depending on whether the space- or the area-filling model is applied. The van der Waals interaction pair potential V_A between two spherical particles of radius R, each surrounded by a solvation layer of thickness δ, may be calculated at a given surface separation of h (i.e., the distance of the centers of mass is $h + 2R + 2\delta$) as in [11–13]:

$$-12V_A = (\sqrt{A_m} - \sqrt{A_s})^2 H_s + (\sqrt{A_s} - \sqrt{A_p})^2 H_p + 2(\sqrt{A_m} - \sqrt{A_s})(\sqrt{A_s} - \sqrt{A_p}) H_{ps} \,, \tag{10}$$

where subscripts m, s and p refer to the dispersion medium, the adsorption layer and the particle, respectively (Fig. 1). The geometric factor H is defined by the following equation [11–13]:

$$H(x,y) = \frac{y}{x^2 + xy + x} + \frac{y}{x^2 + xy + x + y} + 2 \ln\left(\frac{x^2 + xy + x}{x^2 + xy + x + y}\right), \tag{11}$$

where

$$x = \Delta/2R_1, \quad y = R_2/R_1, \quad R_1 \leq R_2$$

$$H_s\text{: } \Delta = h, \quad R_1 = R_2 = R + \delta$$

$$H_p\text{: } \Delta = H + 2\delta, \quad R_1 = R_2 = R$$

$$H_{ps}\text{: } \Delta = h + \delta, \quad R_1 = R, \quad R_2 = R + \delta \,.$$

The Hamaker constants have been tabulated for a number of solid particles and pure liquids [13, 18]. For liquid mixtures, the Hamaker constant can be calculated on the basis of the characteristic frequency (ν_v) and the intrinsic dielectric constant, extrapolated from the visible light range (ε_0) [18]:

$$A = \frac{27}{64} h \nu_v \left(\frac{\varepsilon_0 - 1}{\varepsilon_0 + 2}\right)^2 . \tag{12}$$

The parameters ν_v and ε_0 are determined experimentally by the minimum deviation method [9], based on a linear representation of the wavelength (or frequency, ν) dependence of the refractive index n of the liquid mixtures [18]:

$$\frac{n^2 + 2}{n^2 - 1} = \frac{\varepsilon_0 + 2}{\varepsilon_0 - 1}\left(1 + \frac{\nu^2}{\nu_v^2}\right). \tag{13}$$

The slope and the intercept of the linear function give access to ν_v and ε_0. If the Hamaker constant of the dispersion medium is known as a function of the composition of the medium (A_m vs. x_1), then the Hamaker constant of the interfacial layer as a function of the dispersion medium (A_s vs. x_1) can also be determined via the adsorption equilibrium diagram x_1^s vs. x_1 (Eqs. (4) and (8)). Finally, the van der Waals attraction potential between the particles can be computed according to Eq. (10): either at a given composition, as a function of the distance between the particles, or at a given particle separation, as a function of the composition of the dispersion medium.

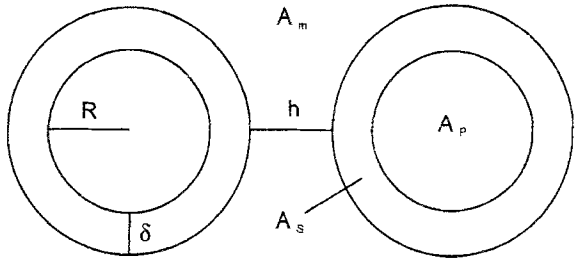

Fig. 1 Solvated hard sphere model (schematic). R: particle radius; δ: thickness of the adsorption layer; h: distance between two approaching particles; A_m, A_p and A_s: Hamaker constants of the dispersion medium, particles and adsorption layer, respectively

Materials and methods

Synthesis of silica particles

Spherical, monodisperse silica particles were prepared by alkaline polycondensation of TEOS (tetraethyl orthosilicate, BDH) according to the method of Stöber [19]. The particle size can be controlled via the concentrations of water, ammonia and TEOS dissolved in ethanol [19–21]. The silica particles obtained were centrifuged and

Colloid & Polymer Science, Vol. 274, No. 8 (1996)

redispersed in ethanol. This purification procedure was repeated until the refractive index of the supernatant liquid was identical with that of pure ethanol. After 5–6 purification cycles, the particles were freeze-dried from dioxane.

Transmission electron microscopy (TEM)

The morphology and size of the silica particles were investigated with an OPTON 902 transmission electron microscopy at 80 kV. A drop of dilute ethanol silica sol was placed on a Formvar grid and, after solvent evaporation, the sample was transferred to the measuring unit of the microscope. Photographs were taken and the size distribution was determined from the micrographs by counting ca. 800–1000 particles.

Photon correlation spectroscopy (PCS)

The size distribution of the particles was also determined with a Sematech dynamic light scattering apparatus. The light source was a He–Ne laser with a power of 5 mW and a wavelength of 632.8 nm. The intensity of the light scattered by the dilute alcosol was detected at an angle of 90° by a photomultiplier coupled with an SEM-633 spectrogoniometer. Data processing was performed by a 12-channel "log–log" correlator (RTG model).

Determination of the BET specific surface area

The specific surface area of the silica particles, a_s(BET), was determined by measuring the adsorption of N_2 at 77 K in a Micromeritics Gemini 2375 automated gas sorption apparatus. Prior to the measurement, the sample was pretreated at 393 K for 2 h at a pressure of $\sim 10^{-3}$ Torr.

Small-angle x-ray scattering (SAXS)

Small-angle x-ray scattering was measured by using CuKα irradiation produced by a Philips PW 1830 x-ray generator at a voltage of 40 kV, a tube current of 35 mA and a wavelength of $\lambda = 0.1542$ nm. The primary beam was led through a Ni-filter into a compact-Kratky camera (Anton Paar, model KCEC/3). The beam width and its thickness were 20 mm and 80 μm, respectively. The powdered sample was pretreated at 393 K in vacuum and placed in a copper sample holder. The alcosol (2 w/v%) was added to a capillary cell. Measurements were made in a He atmosphere for 3 h. The intensity of the scattered radiation was measured by a proportional detector with a slit width of 100 μm in the angle range $2\Theta = 0.06$ to 7°. The measurement was controlled by a PW 1710 microprocessor. The intensity of the scattered radiation was normalized; the absorption of the x-ray beam and background scattering (He or ethanol) were corrected for. The specific surface area of the silica particles, a_s(SAXS), was calculated from the 0th and 1st moments of the corrected scattering function I vs. h, and the surface fractal dimension D_s was computed from the slope of the middle, linear region of the "log–log" representation:

$$a_s(\mathrm{SAXS}) = \frac{4 \cdot 10^3 \Phi_p \Phi_m \int_0^\infty I(h) h dh}{\rho_p \int_0^\infty I(h)\, dh} \tag{14}$$

$$\log(I) \propto (D_s - 5) \log(h)\,, \tag{15}$$

where $h = (4\pi/\lambda) \sin \Theta$ is the scattering vector, Φ_p and Φ_m are the volume fractions of the particles and the medium, respectively, and ρ_p is the density of the particles [22].

Liquid adsorption measurements

2% suspensions were made from ethanol–cyclohexane mixtures and silica powder pretreated at 393 K in a vacuum desiccator. The mixtures were prepared by mass; analytical grade solvents (Reanal, Hungary) dried on a 0.4 μm Merck molecular sieve were used. The samples in Teflon-sealed, screw-capped centrifuge tubes were stirred end-to-end overnight at room temperature. After adsorption equilibrium had been attained, the disperse systems were centrifuged in a Sorvall RC-5B Plus centrifuge at 298 K and the samples were then placed in a 298.15 K water bath for 4 h. The composition of the dispersion medium was analysed in a Zeiss liquid interferometer and a Paar DMA 58 density meter. Adsorption excess amounts were calculated using Eq. (1).

Optical dispersion measurements

The dependence of the refractive index of the liquid pair ethanol–cyclohexane upon wavelength was determined by the minimum deviation method. A Hg–Cd spectral lamp having a line spectrum (SPM-2, Zeiss) was employed as the light source. The angle of minimum deviation (δ_{min}) of the monochromatic light passing through a liquid prism with a refractive angle ψ was determined with the aid of a telescope attached to a high-precision goniometer (MOM). The refractive index of the prism relative to its surroundings was calculated as

$$n_\lambda = \frac{\sin[(\delta_{min} + \psi)/2]}{\sin[\psi/2]}\,. \tag{16}$$

Rotational viscosimetry

The rheological properties of 2% silica suspensions in ethanol–cyclohexane liquid pairs at 298.15 K were investigated in a HAAKE Rotovisco RV-20, CV-100 measuring system. For determination of the τ (shear stress) vs. D (shear rate gradient) flow curves, an ME-30 measuring head and a PG-242 control unit were used. In each case the systems were pre-sheared for 2 min at $D = 100\,s^{-1}$. Measurements were then conducted by progressing from higher shear rates towards lower ones; the duration of one measurement was 2 min.

Results and discussion

The transmission electromicrograph of the silica particles is shown in Fig. 2. The particles are spherical in shape and reasonably monodispersed. Their average diameters obtained by TEM and PCS particle size analysis are $d_p(\text{TEM}) = 198 \pm 15$ nm and $d_p(\text{PCS}) = 204 \pm 20$ nm, respectively. The corresponding differential size distributions are presented in Fig. 3. The geometric surface area calculated from the equation $a_s(\text{GEOM}) = 6000/\rho_p d_p$ is $17\,m^2g^{-1}$. The BET specific surface area was found to be $a_s(\text{BET}) = 43\,m^2g^{-1}$. The results of SAXS measurements are shown in Fig. 4 (for clarity, only counts relating to approximately every eighth scattering angle are displayed). The values obtained for the specific surface area, $a_s(\text{SAXS})$, of the powdered sample and the ethanolic suspension were 47 and $56\,m^2g^{-1}$, respectively (Eq. (14)). By means of SAXS analysis (Eq. (15)), the surface fractal dimension of the particles was calculated from the slopes of the linear sections in Fig. 4. The scattering curves of the particles in the powdered sample and in the silica sol both yielded

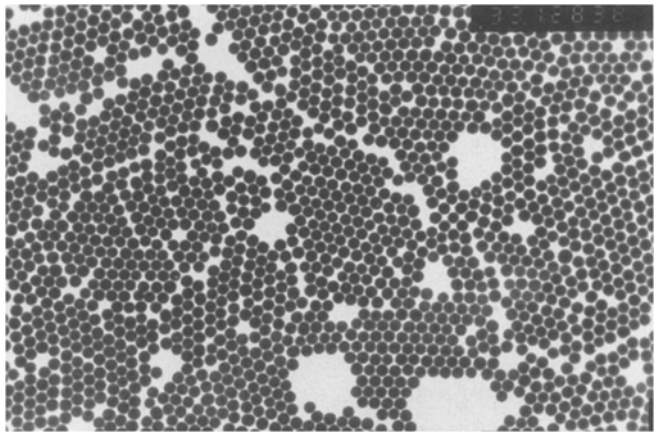

Fig. 2 Transmission electromicrograph of 200 nm Stöber silica particles used in the course of this work

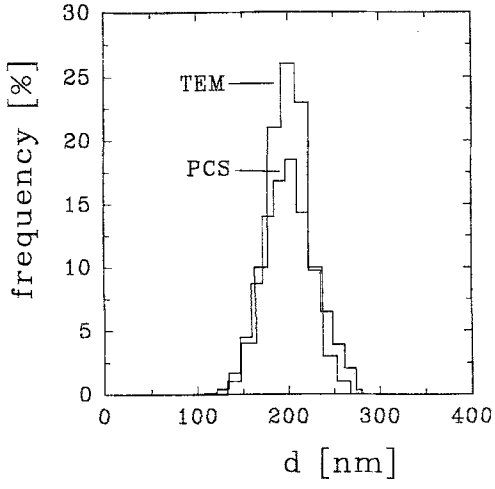

Fig. 3 Particle size distributions of the 200 nm silica particles, obtained from TEM and PCS measurements

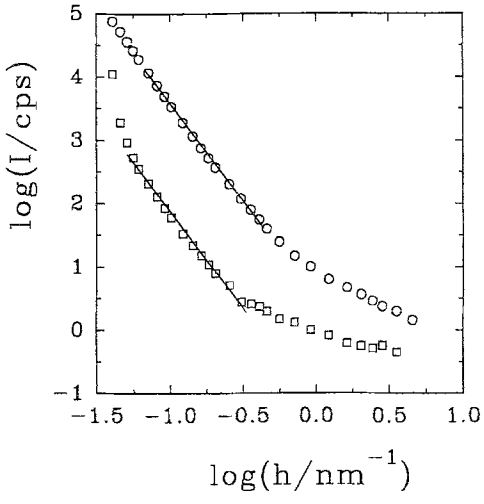

Fig. 4 SAXS functions of the silica particles. (○): silica powder; (□): 2% alcosol

$D_s = 2.04$. (For ideally planar surfaces $D_s = 2$, while for ideally porous materials $D_s = 3$ [22]). The results of TEM, PCS, BET and SAXS measurements show that the surface of the silica spheres is planar (even though not at the molecular level) rather than porous. If the results obtained by means of the various instrumental measurements are averaged and a value of $a_s(\text{av.}) = 48\,m^2g^{-1}$ is accepted for the specific surface area, then the surface roughness has a factor of $r_s = a_s(\text{av.})/a_s(\text{GEOM}) = 2.8$. A large number of data in the literature, based on a comparison of BET surface areas with geometric surface areas of either fumed or precipitated silica particles, likewise indicated roughness factors in the range 2.5–3, irrespective of the history of the preparation [23].

Colloid & Polymer Science, Vol. 274, No. 8 (1996)

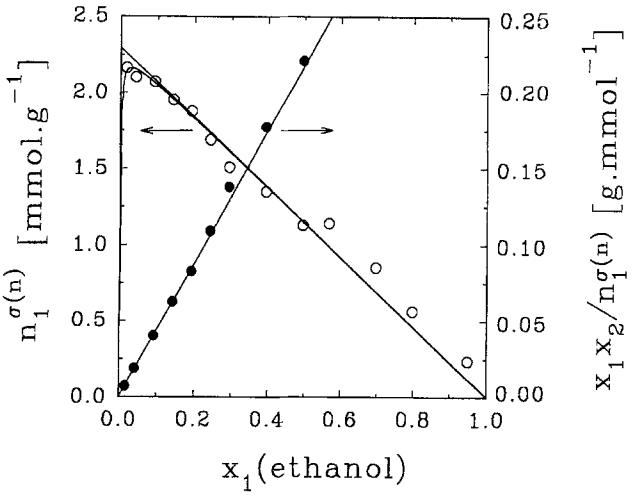

Fig. 5 (○): adsorption excess isotherm of the ethanol (1)–cyclohexane (2)/silica system at 298 K; (●): linear Everett–Schay isotherm-transformation

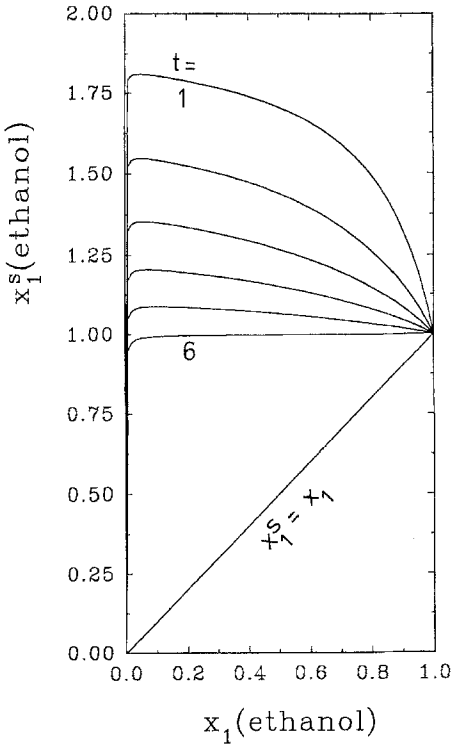

Fig. 6 Equilibrium diagram of the adsorption layer and the dispersion medium in the ethanol(1)–cyclohexane(2)/silica system. Polymolecular adsorption model (Eq. (4)). t indicates the number of layers around the particles

As can be seen in Fig. 5, the adsorption excess isotherm of the ethanol(1)–cyclohexane(2)/Stöber silica system is of type II in the Schay–Nagy classification. The Everett–Schay transformation of the isotherm is also included in the figure. The adsorption of ethanol on the hydrophilic surface is strongly preferential over the adsorption of cyclohexane. The adsorption capacity of ethanol calculated according to the Schay–Nagy extrapolation method (Eq. (2)) or to the linear Everett–Schay representation (Eq. (3)) is 2.30 and 2.28 mmolg^{-1}, respectively. Accordingly, if the molar cross-sectional area of ethanol is taken as $a_1 = 130\ m^2\ mmol^{-1}$ [16, 24], then the area-filling model (left side of Eq. (5)) gives $t = 6.2$ for the number of successive adsorption layers. On the other hand, if the space-filling model is applied (right side of Eq. (5)), a layer number of $t = 5.4$ is obtained, provided that the molar volume of ethanol is $v_1 = 58.4\ cm^2\ mol^{-1}$, and the thickness of a single layer of adsorbed ethanol is $\delta_1 = 0.52$ nm [25]. Generation of the composition of the interfacial layer via Eq. (4), with layer numbers of $t = 1, 2, \ldots, 6$, yields the series of functions shown in Fig. 6. Rusanov's criterion (Eq. (7)) is first obeyed at $t = 6$; this is the minimum number of layers which, in the calculations of the composition of the interfacial layer, leads to a thermodynamically consistent result. An equilibrium diagram corresponding to $t = 6$ in Fig. 6 is also obtained, when the composition of the interfacial layer is calculated via Eq. (8) (the ratio of molar volumes, 108.1/58.4, is practically identical with the ratio of the molar cross-sectional areas [16, 24], 240/130, so that $r = 1.85$).

In summary, it may be stated that in ethanol–cyclohexane mixtures a polymolecular adsorption layer is formed on the surface of 200 nm Stöber silica particles. A value of 6 is a good approximation for the number of layers; hence, the layer thickness is 3.1 nm. The adsorption of ethanol on the hydrophilic surface is strongly preferential. The adsorption equilibrium diagram indicates that, apart from a very narrow, cyclohexane-rich region in the bulk liquid phase, the adsorption layer consists of practically pure ethanol. Although the above-described analysis of the structure of the adsorption layer does contain simplifications, its applicability to calculate the colloid stability of the silica sol can ultimately be accepted or rejected after a comparison with the experimental results (stability behaviour). It is worth mentioning here that statistical thermodynamic calculations on the regular mixture/solid absorbent interface reveal that the polymolecular adsorption layer extends up to 4–7 molecular layers [26]. Model calculations on the stability of colloidal particles dispersed in regular mixtures led to the conclusion that the polymolecular adsorption layer may act in favour of either stability or particle aggregation, depending on the structure of the adsorption layer [27].

Calculation of the van der Waals interaction pair potential between silica particles requires a knowledge of the composition dependence of the Hamaker constant in the

dispersion medium and in the solvation layer; these functions are interrelated via the adsorption equilibrium in the overall system. For this reason, the wavelength dependence of the refractive index of ethanol–cyclohexane mixtures in the entire composition range was determined by the minimum deviation method. The results of these measurements are presented in Fig. 7, in the linearized from described by Eq. (13). The Hamaker constants for the various compositions were calculated from the slopes and intersections of the straight lines according to Eq. (12), while the Hamaker constants of the interfacial layer were computed with the help of the adsorption equilibrium diagram (Fig. 6). The two functions are shown in Fig. 8. Data for pure ethanol and pure cyclohexane are available in the literature [7, 13] and are in excellent agreement with the values reported here. The composition dependence of the Hamaker constant of the liquid pair ethanol(1)–cyclohexane(2) at 298.15 K is described by the following empirical equation: $A_m/kT = 14.320–0.6447x_1 - 2.953x_1^2$. For amorphous silica, the value $A_p = 15.6\,kT$ was taken from the literature [7, 12, 18]. According to Fig. 8, the Hamaker constant of the solvation layer differs considerably from that of the dispersion medium; the values of the functions approach each other only in the ethanol-rich region. Accordingly, if the dominant role in the overall stability of the silica sol is attributed to van der Waals forces, the colloid system may be expected to be stable in a dispersion medium rich in ethanol.

A photograph of the 2% samples used for the determination of the adsorption excess isotherm (Fig. 5) is presented in Fig. 9. The picture was taken after equilibrium had been attained and ca. 20 min after the termination of stirring. Hydrophilic silica is flocculated and

Fig. 7 Frequency dependence of the refractive indices an ethanol(1)–cyclohexane(2) liquid pairs at 298 K according to Eq. (13). Molar fractions ethanol are: 0; 0.05; 0.1; 0.2; 0.3; ... ; 0.8; 0.9; 0.95; 1

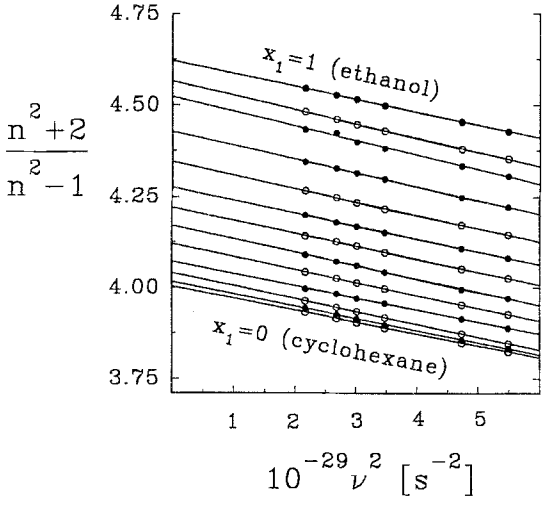

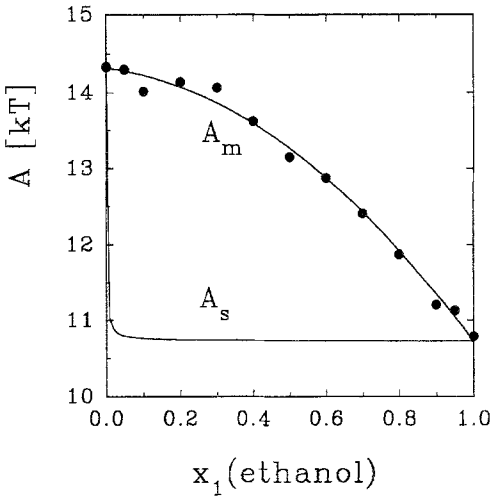

Fig. 8 Composition dependence of the Hamaker constant in the dispersion medium and in the adsorption layer for the ethanol(1)–cyclohexane(2)/silica system

deposited in cyclohexane-rich mixtures, while the silica sol remains stable in the ethanol-rich regime. The critical cyclohexane concentration lies in the molar fraction range 0.4–0.3 (and hence the molar fraction of ethanol is 0.6–0.7). It is important to note that, upon the addition of ethanol, the flocculated system may be redispersed by gentle shaking to give a stable sol again, i.e., the alcosol is reversibly flocculated by the addition of cyclohexane. This indicates that the aggregation of the particles is characterized by a shallow V_{min} potential well, in contrast with a deep primary minimum characteristic of aqueous dispersions coagulated by electrolytes.

Van der Waals attraction potentials, calculated on the basis of Eqs. (10) and (11) as a function of the composition of the dispersion medium, are shown in Fig. 10 for three different interparticle distances. The critical composition of the 2% suspension observed visually (Fig. 9) is indicated by a dashed line; to the right of this boundary (rich in ethanol) the system is stable, while to the left (rich in cyclohexane) it is flocculated. The course of the calculated potential functions is in good agreement with the experimentally observed behaviour. The values (expressed in kT units) likewise seem realistic physically. In the cyclohexane-rich regime, the values of the attraction potential are large with respect to the kinetic energy; the function passes through a maximum attraction towards pure ethanol, and the particle–particle attraction then monotonously decreases. As the composition and the Hamaker constant of the solvation layer approach those of the dispersion medium, the particles are increasingly continuously incorporated into the medium; this harmony can ensure the stability of the overall system, in accordance

Colloid & Polymer Science, Vol. 274, No. 8 (1996)

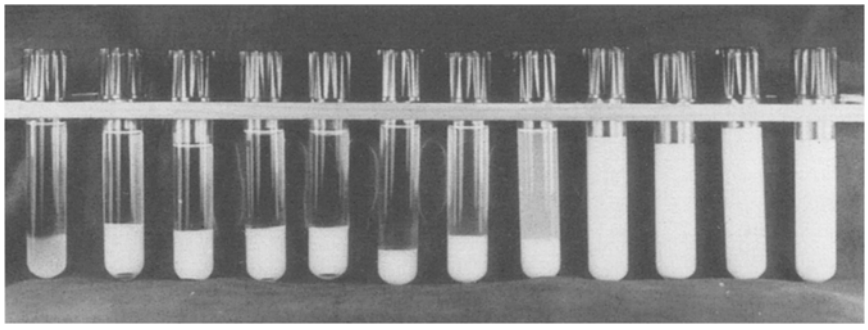

Fig. 9 Photograph of 2% silica dispersions in ethanol(1)–cyclohexane(2) liquid pairs. Molar fractions of ethanol (from left to right): $x_1 = 0$; 0.05; 0.1; 0.2; 0.3; ... ; 0.8; 0.9; 1

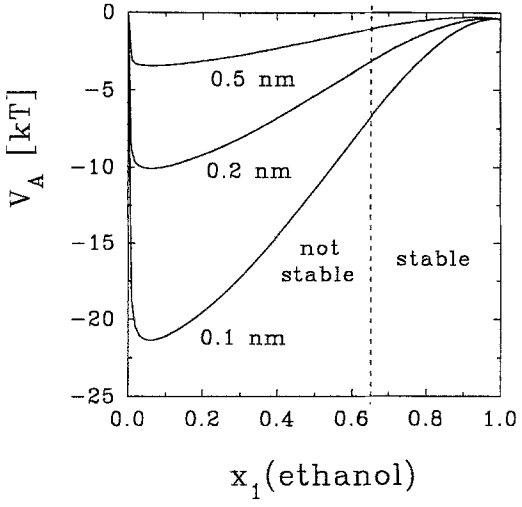

Fig. 10 Van der Waals pair potentials between silica spheres in ethanol(1)–cyclohexane(2) mixtures as a function of composition at fixed particle distances of 0.5, 0.2 and 0.1 nm. The dashed line indicates the flocculated/stable transition zone observed in Fig. 9

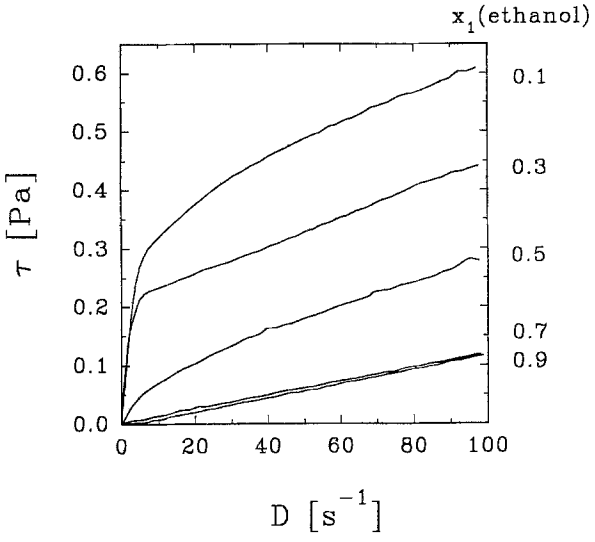

Fig. 11 Flow curves of 2% silica suspensions in ethanol(1)–cyclohexane liquid pairs at 298 K

with the Ostwald–Buzágh theory of continuity [14, 15]. The interparticle interactions, and hence the stability of the colloid system as a whole, are predominantly affected by the solid/liquid interfacial interaction via the structure and composition of the adsorption layer. It should be noted that the attraction potential functions in Fig. 10 are presented for $t = 6$ (i.e., six successive layers of solvent molecules around the particles). This value was also used in pure cyclohexane and for its close proximity (e.g. $x_1 < 0.02$, which corresponds to the ascending region of the adsorption excess isotherm in Fig. 5). In this region the calculated attraction potential predicts a relatively stable silica dispersion, in contrast with visual observations. It is more reasonable to assume, however, that the formation of this thick layer takes place only gradually with increasing ethanol concentration of the bulk liquid phase (up to the beginning of the linear section of the excess isotherm). This argument accounts for the discrepancy between the calculated and the observed stability behaviour in pure cyclohexane and at extremely dilute ethanol concentrations. A gradual building-up of the multilayer is supported by our further model calculations. For example, for $t = 3$ and an equilibrium molar fraction of ethanol of $x_1 = 5 \times 10^{-3}$, the value of the attraction potential for interparticle separations of from 0.5 to 0.1 nm is increased from ca. $-10\,kT$ to $-50\,kT$; these values lie in the unstable region in Fig. 10, in accordance with the experimental observations.

Flow curves of 2% silica dispersions, determined by rotational viscosimetry, are displayed in Fig. 11. In cyclohexane-rich dispersion media, where the adhesion between the particles is high, the flocs are more difficult to break-up; the shear stress (τ) becomes a linear function of the shear rate gradient (D) only after a steeply rising initial section (pseudoplastic behaviour). The slope of this straight line gives the plastic viscosity, η_{pl}, which gradually decreases from 3 to 1 mPas as the system proceeds from pure cyclohexane towards ethanol. The extrapolated intercept is the Bingham yield stress (τ_B), which is a measure of

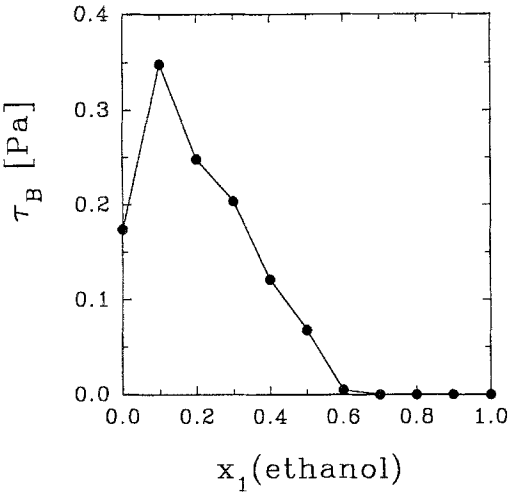

Fig. 12 Dependence of the Bingham yield stress on the composition of the dispersion medium (taken from Fig. 11)

the adhesion between the particles. As the ethanol concentration increases, τ_B, i.e., the attraction between the particles, decreases, and ultimately the aggregate free dispersion behaves as a Newtonian fluid ($\tau_B = 0$). The Bingham yield is plotted against the composition of the dispersion medium in Fig. 12. $\tau_B = 0$ for ethanol molar fractions of ca. $x_1 > 0.65$, which corresponds to the stability domain of the colloidal dispersion. On the other hand, $\tau_B > 0$ for cyclohexane concentrations of $x_2 > 0.35$, where particle aggregates appear in the system. The similarity between the courses of the attraction potential (Fig. 10) and Bingham shear stress (Fig. 12) functions is noteworthy. In fact, τ_B is proportional to the separation energy E_{sep}, i.e., the energy input which leads to the destruction of particle aggregates in a flocculated system [9, 28]; E_{sep} is directly related to the depth of the attraction potential plotted against the interparticle distance. The calculation of E_{sep} from τ_B is critically dependent on the model chosen to describe the aggregation number and structure of the flocs [28, 29]. Application of such a model is not attempted in this work; nevertheless, the qualitative conclusions drawn from the Bingham yields proved satisfactory.

Studies on the electrophoretic mobility of silica particles in organic mixtures, involving checks for trace amounts of water in the medium, are currently in progress. Although the effect of Coulombic forces cannot be ruled out, the agreement between the experimental observations and the model calculations is good, even if the role of the electric double layer is neglected. Further progress can be made by developing a theory which, instead of regarding solvated particles as hard spheres, allows for an incidental overlapping of the solvate layers between colliding particles and takes into account the associated change in local free energy (enthalpy, entropy). Such an overlap model would be particularly applicable to disperse systems in which the particles are surrounded by a thick adsorption layer and the composition of this layer is diffuse from the solid surface towards the bulk liquid phase.

Acknowledgments This work was supported by OTKA grants I/5 T007530 and W015313, and NATO grant CRG 920785.

References

1. Ottewill RH (1973) In: Everett DH (ed) Colloid Science, Specialist Periodical Reports, Vol 1. The Chemical Society, London, Chap 5
2. Overbeek JTh (1982) In: Goodwin JW (ed) Colloidal Dispersions. The Royal Society of Chemistry, London, Chap 1
3. Kline SR, Kaler EW (1994) Langmuir 10:412
4. Beysens D, Esteve D (1985) Phys Rev Letters 54:2123
5. Gurfein V, Beysens D, Perrot F (1989) Phys Rev A 40:2543
6. Edwards J, Everett DH, O'Sullivan T, Pangalou I, Vincent B (1984) J Chem Soc Faraday Trans I 80:2599
7. Vincent B, Király Z, Emmett S, Beaver A (1990) Coll Surf 49:121
8. Machula G, Dékány I (1991) Coll Surf 61:331
9. Machula G, Dékány I, Nagy LG (1993) Coll Surf 71:241
10. Dékány I (1993) Pure Appl Chem 65:901
11. Vold MJ (1961) J Colloid Sci 16:1
12. Osmond DWJ, Vincent B, Waite FAW (1973) J Colloid Interface Sci 42:262
13. Vincent B (1973) J Colloid Interface Sci 42:270
14. Buzágh A (1952) Colloid Chemistry. Vol 2/1, Akadémiai Kiadó, Budapest, p 29 (in Hungarian)
15. Szántó F (1987) Fundamentals of Colloid Chemistry. Gondolat, Budapest, p 137 (in Hungarian)
16. Schay G, Nagy LG (1974) Adsorption from Solution at the Solid/Liquid and Liquid/Vapour Interface. Advances in Chemistry. Vol 18, Akadémiai Kiadó, Budapest, Chap 4 (in Hungarian)
17. Everett DH (1973) In: ref. 1 Chap 2
18. Gregory J (1969) Adv Colloid Interface Sci 2:396
19. Stöber W, Fink A, Bohn E (1968) J Colloid Interface Sci 26:62
20. van Helden AK, Jansen JW, Vrij A (1982) J Colloid Interface Sci 81:354
21. Bogush GH, Tracy MA, Zukoski CF (1988) J Non-Cryst Solids 104:95
22. Turi L, Dékány I (1995) In: Proc. 6th Symp. Particle Size Analysis, Environmental and Powder Technology (Győr), MATE, Budapest, p 85
23. Gregg SJ, Sing KSW (1967) Adsorption, Surface Area and Porosity. Academic, London, New York, Chap 2
24. McClellan AL, Harnsberger HF (1967) J Colloid Interface Sci 23:577
25. Gregg SJ, Sing KSW (1967) In: ref. 23 p 203
26. Lane JE (1968) Aust J Chem 21:827
27. Ash SG (1974) J Chem Soc Faraday Trans II 70:895
28. Firth BA, Hunter RJ (1976) J Colloid Interface Sci 57:248
29. Firth BA, Hunter RJ (1976) J Colloid Interface Sci 57:266